Inorg. Chem. **2007**, *46*, 1337−1342

Two 3D Porous Lanthanide−Fumarate−Oxalate Frameworks Exhibiting Framework Dynamics and Luminescent Change upon Reversible De- and Rehydration

Wen-Hua Zhu, Zhe-Ming Wang,* and Song Gao*

Beijing National Laboratory for Molecular Sciences, State Key Lab of Rare Earth Materials Chemistry and Applications, College of Chemistry and Molecular Engineering, Peking University, Beijing 100871, People's Republic of China

Received September 26, 2006

We present two porous luminescent compounds, $[Ln_2(fumarate)_2(oxalate)(H_2O)_4]\cdot 4H_2O$ (Ln = Eu, Tb), prepared by the hydrothermal method. The materials have 3D framework structure consisting of oxalate pillared lanthanide−fumarate layers with intersected channels occupied by guest water. They exhibit framework dynamics upon several cycles of dehydration and rehydration. The crystallinity of the as-prepared hydrated materials degrades completely to the amorphous dehydrated phases, while it returns upon rehydration. A mechanism for de-/rehydration is proposed on the basis of the structure and spectroscopic data. The dehydration process is accompanied by the lost of luminescence of Ln ion, but the luminescence is recovered upon rehydration, where water molecules in fact enhance the luminescence but not quench it. This is probably due to the softened environment of lanthanide ion in the dehydrated amorphous phases and the recovery of the stiffness after rehydration.

Introduction

With great attention paid to porous metal−organic frameworks (PMOFs) and the excellent achievements obtained on their fascinating structures and conventional applications in gas storage, separation, catalysis, etc., directly related to the porosity,[1] other aspects of these PMOFs, such as the framework dynamics[1a,2] and guest-sensitive properties,[3,4] have become the new focus in the area. The attempt to combine porosity with other properties of PMOFs will lead to finding new phenomena and creating new multifunctional materials. In this context, PMOFs containing lanthanide (Ln) ions are attractive because of their versatile coordination chemistry, their unique luminescent and magnetic properties, and possible high framework stability.[5] To date, few examples of guest-dependent luminescent property of lanthanide PMOFs have been reported. Such materials have the potential in applications such as guest sensing and recognition because they can have a luminescent response to guest absorption and exchange.[6] To exploit luminescent PMOFs, we chose Eu^{3+}/Tb^{3+}−fumarate−oxalate systems in this study. Eu^{3+} and Tb^{3+} are the two most common lanthanide luminophores. Fumarate (fum) is a unique ligand with a relatively small,

* To whom correspondence should be addressed. Phone: 86-10-62755926. Fax: 86-10-62751708. E-mail: zmw@pku.edu.cn (Z.-M.W.), gaosong@pku.edu.cn (S.G.).

(1) For recent reviews, see: (a) Kitagawa, S.; Kitaura, R.; Noro, S. *Angew. Chem., Int. Ed.* **2004**, *43*, 2334 and references therein. (b) Rowsell, J. L. C.; Yaghi, O. M. *Angew. Chem., Int. Ed.* **2005**, *44*, 4670 and references cited therein. (c) Reed, C. A., Ed. Special issue on Molecular Architectures. *Acc. Chem. Res.* **2005**, *38*, 215. (d) O'Keeffe, M., Yaghi, O. M., Eds. Special issue on Reticular Chemistry. *J. Solid State Chem.* **2005**, *178*, 2409.

(2) (a) Kitagawa, S.; Uemura, K. *Chem. Soc. Rev.* **2005**, *34*, 109 and references cited therein. (b) Uemura, K.; Matsuda, R.; Kitagawa, S. *J. Solid State Chem.* **2005**, *178*, 2420 and references cited therein.

(3) (a) Kepert, C. J. *Chem. Commun.* **2006**, 695 and references cited therein. (b) Maspoch, D.; Ruiz-Molina, D.; Veciana, J. *J. Mater. Chem.* **2004**, 2713 and references cited therein.

(4) For example: (a) Halder, G. J.; Kepert, C. J.; Moubaraki, B.; Murray, K. S.; Cashion, J. D. *Science* **2002**, *298*, 1762. (b) Kurmoo, M.; Kumagai, H.; Chapman, K. W.; Kepert, C. J. *Chem. Commun.* **2005**, 3012. (c) Maspoch, D.; Ruiz-Molina, D.; Wurst, K.; Domingo, N.; Cavallini, M.; Biscarini, F.; Tejada, J.; Rovira, C.; Veciana, J. *Nat. Mater.* **2003**, *2*, 190. (d) Wang, Z.-M.; Zhang, B.; Fujiwara, H.; Kobayashi, H.; Kurmoo, M. *Chem. Commun.* **2004**, 416. (e) Kurmoo, M.; Kumagai, H.; Akita-Tanaka, M.; Inoue, K.; Takagi, S. *Inorg. Chem.* **2006**, *45*, 1627.

(5) For example: (a) James, S. L. *Chem. Soc. Rev.* **2003**, *32*, 276. (b) Sun, Y.-Q.; Zhang, J.; Chen, Y.-M.; Yang, G.-Y. *Angew. Chem., Int. Ed.* **2005**, *44*, 5814. (c) Maji, T. K.; Mostafa, G.; Chang, H.-C.; Kitagawa, S. *Chem. Commun.* **2005**, 2436. (d) Pan, L.; Adams, K. M.; Hernandez, H. E.; Wang, X.; Zheng, C.; Hattori, Y.; Kaneko, K. *J. Am. Chem. Soc.* **2003**, *125*, 3062. (e) Devic, T.; Serre, C.; Audebrand, N.; Marrot, J.; Férey, G. *J. Am. Chem. Soc.* **2005**, *127*, 12788.

(6) (a) Bai, Y.; He, G.-J.; Zhao, Y.-G.; Duan, C.-Y.; Dang, D.-B.; Meng, Q.-J. *Chem. Commun.* **2006**, 1530. (b) Mitchell-Koch, J. T.; Borovik, A. S. *Chem. Mater.* **2003**, *15*, 3490.

10.1021/ic061833e CCC: $37.00
Published on Web 01/18/2007

conjugated middle part of CH═CH and versatile coordination modes, allowing possible porosity in the constructed framework.[7,8] In our previous work,[8] we have demonstrated that PMOFs of the fum-pillared Ln−fum layer structure can be obtained for the middle Ln ions, and they show interesting reversible de-/rehydration processes and framework dynamics, while oxalate (ox) has been proved to be a good bridging ligand in constructing PMOFs.[9] Reported here are two new isostructural Ln−fum−ox compounds, $[Ln_2(fum)_2(ox)(H_2O)_4]\cdot 4H_2O$ (Ln = Eu, **1Eu** and Ln = Tb, **2Tb**). They are porous ox-pillared Ln−fum layer structures with intersected channels occupied by water molecules. Interestingly, the materials exhibit reversible de-/rehydration processes, and the as-prepared, dehydrated, and rehydrated ones show large changes in their luminescent properties.

Experimental Section

Synthesis and De-/Rehydration Experimental Details. All starting materials were commercially available reagents of analytical grade and used without further purification. Preparation for **1Eu**: a mixture of $Eu(NO_3)_3\cdot 6H_2O$ (0.178 g, 0.40 mmol), fumaric acid (0.142 g, 1.2 mmol), oxalic acid (0.025 g, 0.20 mmol), and H_2O (10 mL) was sealed in a Teflon-lined stainless steel vessel (23 mL) and heated at 150 °C for 2 days. Crystals of **1Eu** were harvested in a yield of 86% based on Eu salt. Anal. Calcd for $C_{10}H_{20}O_{20}Eu_2$: C, 15.72; H, 2.64. Found: C, 15.64; H, 2.64. Preparation for **2Tb**: the compound was prepared by a similar method, using $Tb(NO_3)_3\cdot 6H_2O$. Yield 90%. Anal. Calcd for $C_{10}H_{20}O_{20}Tb_2$: C, 15.44; H, 2.59. Found: C, 15.67; H, 2.56. The phases of dehydrated **1Eu** and **2Tb** were obtained by heating samples of **1Eu** and **2Tb** at 120 °C under a dynamic vacuum (10^{-2} Torr) for 1 day. Anal. Calcd for $C_{10}H_4O_{12}Eu_2$: C, 19.37; H, 0.65. Found: C, 19.39; H, 0.94. For $C_{10}H_4O_{12}Tb_2$: C, 18.95; H, 0.64. Found: C, 18.41; H, 1.17. The rehydration of the dehydrated phases was performed by exposing the dehydrated samples of **2Tb** to vapor of water in sealed vessels overnight or directly dropping water onto the dehydrated samples of **1Eu** in air. The de-/rehydration was performed for five cycles.

X-ray Crystallography Study. Crystallographic data for single crystals of **1Eu** and **2Tb** were collected[10] at room temperature on a Nonius Kappa CCD diffractometer with a 2.0 kW sealed tube source using graphite monochromated Mo Kα radiation of λ = 0.71073 Å. Empirical absorption[11] corrections were applied using the Sortav program.[10b] The structures were solved by the direct method and refined by the full-matrix least-squares method on F^2 with anisotropic thermal parameters for all non-hydrogen atoms, using the SHELX program.[12] Hydrogen atoms of the coordinated water molecule were added by difference Fourier map and refined isotropically with constrains for the ideal geometry of water molecule with an O−H distance of 0.96 Å and an H−O−H angle of 105°. Hydrogen atoms attaching to C of fum were added by calculation positions. Hydrogen atoms of the lattice water were not included. Crystallographic data are given in Table 1, and selected bond distances are in Table 2. Powder X-ray diffraction (PXRD) patterns for the as-prepared, dehydrated, and rehydrated samples, and the residues of **1Eu** and **2Tb** heated at 600 °C in air for several hours, were obtained on a Rigaku D/max 2000 diffractometer at room temperature with Cu Kα radiation in a flat plate geometry.

Physical Measurements. Elemental analyses (C, H) were performed on an Elementar Vario EL analyzer. FTIR spectra were recorded on a Nicolet Magna-IR 750 spectrometer equipped with a Nic-Plan microscope against the pure samples in the range of 4000−650 cm^{-1}. Thermal analyses, TGA, and DTA were performed on a SDT 2960 Thermal Analyzer at a heating rate of 5 °C/min under air. The luminescence spectra of as-prepared, dehydrated, and rehydrated samples were recorded on a Hitachi

Table 1. Crystallographic Data for **1Eu** and **2Tb**

	1Eu	2Tb
formula	$C_{10}H_{20}Eu_2O_{20}$	$C_{10}H_{20}O_{20}Tb_2$
molecular weight	764.18	778.10
temperature, K	293	293
crystal system	orthorhombic	orhorhombic
space group	*F ddd*	*F ddd*
a, Å	9.6976(2)	9.6648(2)
b, Å	15.4428(4)	15.4844(3)
c, Å	27.4205(6)	27.1305(6)
α, deg	90	90
β, deg	90	90
γ, deg	90	90
V, Å^3	4106.4(2)	4060.2(2)
Z	8	8
D_c, g/cm^3	2.472	2.546
μ (Mo Kα), mm^{-1}	6.152	7.010
crystal size, mm^3	0.19 × 0.17 × 0.12	0.28 × 0.27 × 0.25
max and min transmission	0.480, 0.332	0.207, 0.119
θ_{min}, θ_{max}, deg	4.46, 27.49	4.48, 27.47
total reflections collected	15 956	17 548
unique reflections (R_{int})	1180 (0.0749)	1167 (0.0734)
observed reflections [$I \geq 2\sigma(I)$]	882	952
no. of refined parameters	82	82
R1,wR2 [$I \geq 2\sigma(I)$]	0.0275, 0.0607	0.0212, 0.0542
R1,wR2 (all data)	0.0455, 0.0641	0.0294, 0.0563
GOF	0.974	1.034
max and min residual density, e/Å^3	0.777, −1.902	0.966, −0.899
max and mean shift/σ	0.001, 0.000	0.001, 0.000

Table 2. Selected Bond Distances (Å) for **1Eu** and **2Tb**[a]

	1Eu	2Tb
Ln(1)−O(1)$^{\#1}$	2.371(3)	2.329(2)
Ln(1)−O(1)$^{\#2}$	2.371(3)	2.329(2)
Ln(1)−O(2)	2.487(3)	2.456(3)
Ln(1)−O(2)$^{\#3}$	2.487(3)	2.456(3)
Ln(1)−O(3)	2.454(3)	2.430(2)
Ln (1)−O(3)$^{\#3}$	2.454(3)	2.430(2)
Ln(1)−O(4)	2.478(3)	2.456(3)
Ln(1)−O(4)$^{\#3}$	2.478(3)	2.456(3)
Ln(1)−O(1)	2.944(3)	2.993(3)
Ln(1)−O(1)$^{\#3}$	2.944(3)	2.993(3)
O(1)−C(1)	1.248(5)	1.241(4)
O(2)−C(1)	1.255(6)	1.262(4)
O(3)−C(3)	1.247(4)	1.247(3)
C(1)−C(2)	1.483(7)	1.493(5)
C(2)−C(2)$^{\#4}$	1.276(10)	1.298(8)
C(3)−O(3)$^{\#5}$	1.247(4)	1.247(3)
C(3)−C(3)$^{\#3}$	1.532(12)	1.545(9)

[a] Symmetry codes: #1 $-x+1, -y, -z+1$; #2 $x+{}^1/_4, y+{}^1/_4, -z+1$; #3 $-x+{}^5/_4, -y+{}^1/_4, z$; #4 $-x+{}^1/_4, -y+{}^1/_4, z$; #5 $-x+{}^5/_4, y, -z+{}^5/_4$.

(7) (a) Michaelides, A.; Skoulika, S.; Bakalbassis, E. G.; Mrozinski, J. *Cryst. Growth Des.* **2003**, *3*, 487. (b) Serre, C.; Pelle, F.; Gardant, N.; Férey, G. *Chem. Mater.* **2004**, *16*, 1177.

(8) Zhu, W.-H.; Wang, Z.-M.; Gao, S. *Dalton Trans.* **2006**, 765.

(9) (a) Song, J.-L.; Mao, J.-G. *Chem.-Eur. J.* **2005**, *11*, 1417. (b) Vaidhyanathan, R.; Natarajan, S.; Rao, C. N. R. *J. Solid State Chem.* **2004**, *177*, 1444.

(10) (a) "Collect" data collection software; Nonius B.V.: Delft, The Netherlands, 1998. (b) "HKL2000" and "maXus" softwares; University of Glasgow, Scotland, UK; Nonius B.V.: Delft, The Netherlands and MacScience Co. Ltd.: Yokohama, Japan, 2000.

(11) (a) Blessing, R. H. *Acta Crystallogr.* **1995**, *A51*, 33. (b) Blessing, R. H. *J. Appl. Crystallogr.* **1997**, *30*, 421.

(12) (a) Sheldrick, G. M. *SHELXTL*, Version 5.1; Bruker Analytical X-ray Instruments Inc.: Madison, WI, 1998. (b) Sheldrick, G. M. *SHELX-97*, PC Version; University of Göttingen: Germany, 1997.

Table 3. IR Absorption Bands (cm^{-1}) and Their Assignments for **1Eu**, **2Tb**, and Their Dehydrated Phases[a]

vibrations	**1Eu**	dehydrated **1Eu**	**2Tb**	dehydrated **2Tb**
C/O−H str	3700−2800 br, s	3084 vw	3700−2900 br, s	3080 vw
		2955 vw		2988 vw
COO str, asym (ox) & C=C str (fum)	1672 s, 1650 s	1656 s	1675 s, 1649 s	1667 s
COO str, asym (fum)	1564 vs	1558 s	1564 vs	1558 vs
COO str, sym (fum & ox)	1412 vs	1401 s	1411 vs	1401 vs
O−H bending	1350 m		1353 m	
δ C−H (?)	1316 w	1313 w	1317 w	1312 w
ν_8 COO	1280 sh, w	1277 sh, w	1284 sh, w	1274 sh, w
	1227 m	1212 m	1220 m	1213 m
ν_6 COO oop def	1095 vw	1090 vw	1090 vw	1100 vw
C−H oop def	986 m	975 m	986 m	975 m
ν_3 COO	904 vw	898 vw	905 vw	896 vw
ν_9 COO def, sym	806 m	800 m	807 m	802 m
γ_{aq}	692 m		691 m	
C−H oop def (?)	669 sh, w	668 w	668 sh, w	668 w

[a] vs, very strong; s, strong; m, medium; w, weak; vw, very weak; sh, shoulder; br, broad; str, stretching; asym, asymmetric; sym, symmetric; oop, out of plane; def, deformation.

F-4500 spectrophotometer at room temperature, under the same instrument and measurement conditions for each batch sample.

Results and Discussion

Synthesis and IR Spectra. The hydrothermal reaction of the lanthanide nitrate, fumaric, and oxalic acids at 150 °C produced the crystals of two isostructural compounds in ca. 90% yield. It is of interest to note that the compounds contain both fum and ox ligands, and this was rarely observed before for lanthanide frameworks to our best knowledge, although few examples of lanthanide frameworks with oxalate and some other carboxylates have been reported.[9] It is well known that lanthanide ions are easily precipitated by oxalate, but under the condition of hydrothermal synthesis the preparation of new lanthanide frameworks containing both oxalate and other ligands is possible, as demonstrated by this work and other reports.[9]

The IR spectra of **1Eu** and **2Tb** and their dehydrated phases are presented in Figure S1, and the bands assignments[13] are given in Table 3. The similarity reflects the isostructural characteristics of the compounds discussed later. For the as-prepared compounds, the broad bands of 3700−2800 cm^{-1} characterize water in the structures, although these bands contain weak C−H stretching. O−H bending at 1350, 1353 cm^{-1} and γ_{aq} for water at 692, 691 cm^{-1} are observed. These bands disappear on the spectra of dehydrated phases, leaving weak bands of C−H stretching at ca. 3000 cm^{-1}. Strong bands of 1700−1400 cm^{-1} are characteristic of COO groups. Bands at ca. 1660 and 1560 cm^{-1} are asymmetric stretching of COO of ox and fum, respectively, and that at ca. 1410 cm^{-1} is from symmetric stretching of COO. Bands at 1660 cm^{-1} should involve vibrations of C=C of fum. The remaining medium or weak bands are deformation, etc., of COO and C−H groups. It is worth noting that band shift to lower wavenumbers is observed for the dehydrated phases as compared to the as-prepared materials, and this should be related to the dehydration mechanism (see later).

Description of Structures of 1Eu and 2Tb. The two compounds are iso-structural, possessing a 3D porous framework of ox-pillared Ln−fum layers (Figure 1). The unique Ln ion is 8-fold coordinated by four fum's (two anti-O and two syn-O), two water, and one bis-chelating ox, in a bi-capped trigonal prism (Figure 1a). The Ln−O bond lengths (Table 2) are 2.369−2.488 Å for **1Eu** and 2.330−2.457 Å for **2Tb**, respectively, seemingly typical for lanthanide carboxylates,[5] and in good agreement with the ionic radii of the two Ln ions, smaller for Tb^{3+} than for Eu^{3+}. In the secondary coordination sphere of the Ln ion, there are two oxygen atoms, O1 and O1$^{\#3}$ at ($-x + {}^5/_4$, $-y + {}^1/_4$, z) from the fum ligand (Figure 1a), with Ln−O distances of 2.944 (**1Eu**) and 2.993 (**2Tb**) Å, and they might be related to the de-/rehydration mechanism and the luminescent property of the materials discussed later. The Ln−fum layer extends in the *ab* plane (Figure 1b), and the Ln ions are linked into chain by two syn−anti COO bridges along one diagonal direction ($a+b$), then the neighboring parallel chains are connected along the other diagonal direction ($a-b$), with the intra- and interchain Ln−Ln separations being 4.5 and 8.2−9.7 Å, respectively. The two coordination waters and the ox of each Ln ion stretch out of the Ln−fum layer, with the water pair on one side and the ox on the other side, but their orientations are opposite for the neighboring Ln ion. Along the *c* direction, the Ln−fum layers are pillared by the ox, thus resulting in a 3D framework (Figure 1c−e), where the interlayer Ln−Ln distance via ox is ca. 6.3 Å.

The 3D framework has channels, as expected for a pillared layer structure,[2] along the *a*, $a+b$, and $a-b$ directions (Figure 1c−e), and they are intersected. The channels are occupied by lattice water molecules, that is, four per formula. The framework possesses a solvent accessible volume[14] of ca. 400 $Å^3$, 10% of the unit cell. However, as the coordination water molecules protrude into the interlayer region, they in fact block the channels along the *a* direction, and the openness of channels along the two diagonal directions is

(13) (a) Williams, D. H.; Fleming, I. *Spectroscopic Method in Organic Chemistry*, 5th ed.; Beijing World Publishing Corporation/ McGraw-Hill: Beijing, China, 1998. (b) Nakamoto, K. *Infrared and Raman Spectra of Inorganic and Coordination Compounds*; Wiley: New York, 1986. (c) Viertelhaus, M.; Henke, H.; Anson, C. E.; Powell, A. K. *Eur. J. Inorg. Chem.* **2003**, 2283. (d) Stoilova, D.; Koleva, V. *J. Mol. Struct.* **2000**, *553*, 131.

(14) Spek, A. L. *PLATON, A Multipurpose Crystallographic Tool*; Utrecht University: The Netherlands, 2001.

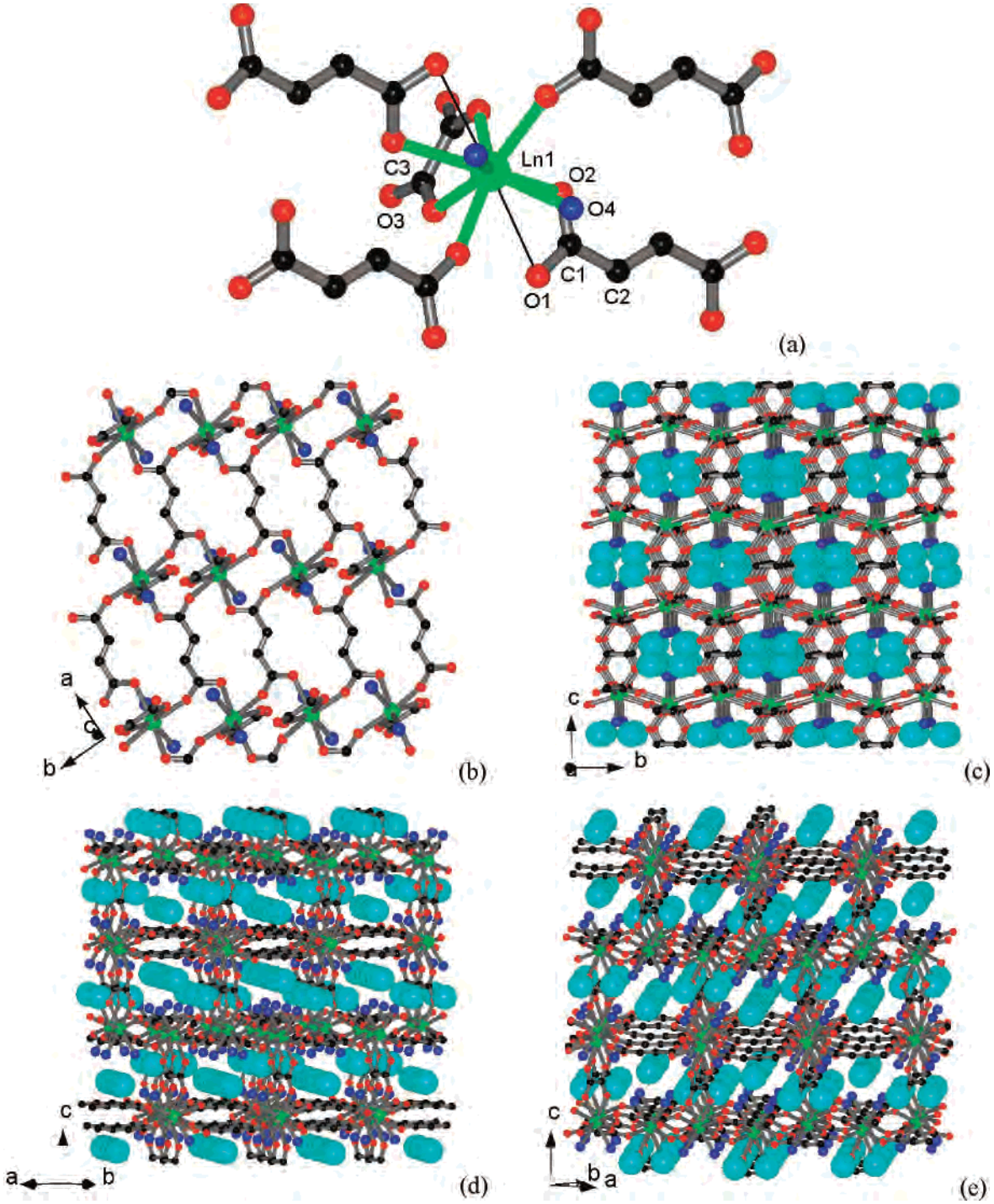

Figure 1. The structure of $[Ln_2(fum)_2(ox)(H_2O)_4]\cdot 4H_2O$. (a) Local coordination environment of Ln ion. The two black thin bonds are the two long Ln−O1 bonds. (b) One Ln-fum layer. (c−e) The views of the 3D porous framework viewed along the *a* axis, *a*+*b* direction, and *a*−*b* direction. Color scheme: Ln, green; C, black; O of fum and ox, red; the coordination water, blue; and the lattice water, cyan. H atoms are omitted for clarity.

ca. 3 × 7 Å estimated with the exclusion of the vdW radii of the surface atoms. The lattice water molecules are supported by the coordination water and COO groups of the framework via H-bonds, with O···O distances of ca. 2.8 Å. The lattice water molecules also form H-bonded dimer with O···O distances of 2.75 Å.

Thermal Property and De-/Rehydration Behavior. The two as-prepared compounds experienced two similar thermal processes in TGA-DTA runs under air (Figure 2). The first endothermic one occurs at ca. 140 °C, but showing continuing weight loss below 120 °C and tailing till 280 °C. Regarding the porous structures, the lattice water might escape before the coordination ones in the first thermal process, although no distinct two steps are observed. The total weight losses are 17.8% (**1Eu**) and 18.5% (**2Tb**), in agreement with the calculated value of 18.9% (**1Eu**) and 18.5% (**2Tb**) for the total 8 water molecules per formula. The second exothermic process at ca. 450 °C is the decomposition of the dehydrated phases. The final residues, 46.1% (**1Eu**) and 47.7% (**2Tb**), are close to the 46.0% based

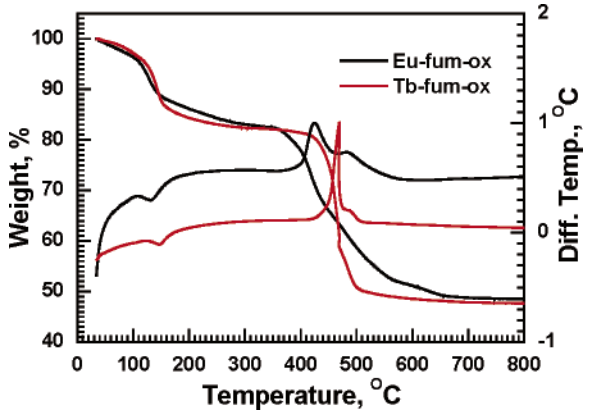

Figure 2. Combined TGA−DTA runs on **1Eu** and **2Tb** under air flow.

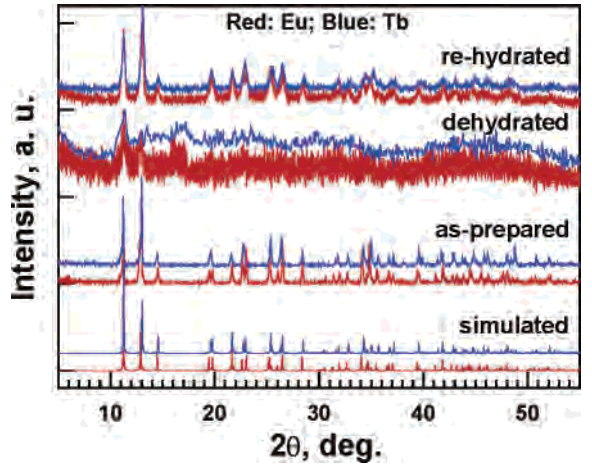

Figure 3. Powder X-ray diffraction patterns of **1Eu** and **2Tb**, their dehydrated and rehydrated phases, and the simulated ones based on the single-crystal structure of the as-prepared compounds.

on Eu_2O_3 and 48.0% based on Tb_4O_7, respectively. The residues after thermal decomposition, identified by the PXRD (Figure S2), are the body-centered cubic Eu_2O_3 and face-centered cubic Tb_4O_7, respectively.[15]

To investigate if the materials are robust to guest removal or exchange, their dehydration and rehydration were studied, and PXRD was used to check the phases. The as-prepared materials were heated at 120 °C under a dynamic vacuum (10^{-2} Torr) for 1 day, leading to a weight loss of 17.1% and 18.3% for **1Eu** and **2Tb**, respectively. This corresponds to nearly complete loss of water, as evidenced by IR spectra (Table 3 and Figure S1), where the bands corresponding to water disappear in the spectra of the dehydrated phases, and the elemental analysis results (Experimental Section). The dehydrated phases, with a formula of $[Ln_2(fum)_2(ox)]$, have almost featureless PXRD patterns (Figure 3). This indicated that they are very low crystalline or amorphous, resulting from the loss of coordination water and probable collapse of the open frameworks.[2] However, when the dehydrated phases were exposed to water vapor at room temperature for 1 day, the two samples gained their original weights, and recovered the original structures, as indicated by comparing their PXRD patterns to the as-prepared ones (Figure 3). Consequently, the dehydration and rehydration are reversible for the materials, and the porous frameworks show framework dynamics[1a,2] upon de-/rehydration. This is similar to our previously reported Ln−fum PMOF system[8] and other Ln PMOFs.[16] In the subsequent four cycles of de-/rehydration, the weight lossses for rehydrated **1Eu** and **2Tb** upon dehydration were successively 16.1%, 8.2%, 8.1%, 7.7% and 17.0%, 16.3%, 13.8%, 12.9%, and the weight gains for dehydrated **1Eu** and **2Tb** upon rehydration were successively 9.0%, 8.7%, 8.3%, 7.6% and 16.7%, 15.7%, 14.9%, 13.6%. The half water upload for the dehydrated Eu series might be due to the faster evaporation of dropped water than rehydration of the dehydrated samples open to air (see Experimental Section). At the same time, the dehydrated phases showed featureless PXRD patterns and low X-ray scattering ability, while the rehydrated materials have PXRD patterns similar to those of the as-prepared materials (Figure S3). The line width of the first rehydrated phase increased significantly as compared to the as-prepared samples; however, no further obvious broadening of line width was observed in the subsequent de-/rehydration cycles. Therefore, the two materials were basically reversible upon five cycles of de-/rehydration, although some degradation might occur.

The dehydration or rehydration might occur through the open channels in the frameworks,[2,8] and during dehydration the two oxygen atoms (O1 and O1$^{\#3}$ of fum, Figure 1a) of the secondary coordination sphere of the Ln ion might enter into the first coordination sphere, with the departure of the coordination water, and vice versa. The dehydrated frameworks should structurally be closely related to its parents. The bond exchange between $Ln-O_{water}$ and $Ln-O_{COO}$ has been documented in some previous reports.[8,16a,b,17] The shift of those bands of the carboxylato group, several or ten cm^{-1} to lower wavenumbers (Table 3 and Figure S1), seemingly supports this mechanism. This mechanism, which needs to be proved further, can explain the de-/rehydration reversibility of the materials.

Luminescence upon De-/Rehydration Procedure. The luminescent properties of the two materials, upon the de- and rehydration processes, are shown in Figure 4. Excited at 394 nm, **1Eu** exhibited red luminescence (Figure 4a), with emissions characterizing $^5D_0 \rightarrow {}^7F_J$ ($J = 0-4$) transitions of Eu^{3+}.[18] The strongest emission of the $^5D_0 \rightarrow {}^7F_2$ transition at 617 nm is 4 times stronger than the second one of the $^5D_0 \rightarrow {}^7F_1$ transition at 591 nm, indicating noncentrosymmetric Eu^{3+} site in **1Eu**,[18] as the structure revealed. However, the dehydrated **1Eu** shows luminescence with intensity only a few percent or less than that of **1Eu**, and the rehydrated sample recovers the luminescence intensity to the same order as the parent one. The excitation spectrum (Figure 4b) behaves similarly. **2Tb** emits green light when excited at

(15) I-centered cubic Eu_2O_3, ICSD#40472; F-centered cubic Tb_4O_7, ICSD#28916.

(16) (a) Pan, L.; Zheng, N.; Wu, Y.; Han, S.; Yang, R.; Huang, X.; Li, J. *Inorg. Chem.* **2001**, *40*, 828. (b) Michaelides, A.; Skoulika, S. *Cryst. Growth Des.* **2005**, *5*, 529. (c) Kiritsis, V.; Michaelides, A.; Skoulika, S.; Golhen, S.; Ouahab, L. *Inorg. Chem.* **1998**, *37*, 3407.
(17) Serre, C.; Millange, F.; Marrot, J.; Férey, G. *Chem. Mater.* **2002**, *14*, 2409.
(18) Vicentini, G.; Zinner, L. B.; Zukerman-Schpector, J.; Zinner, K. *Coord. Chem. Rev.* **2000**, *196*, 353.

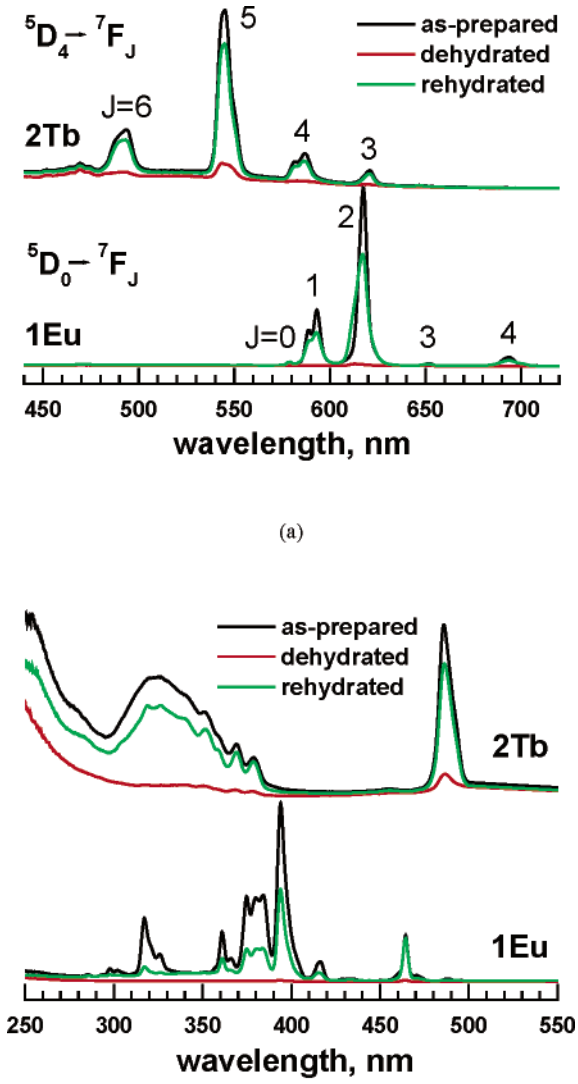

Figure 4. The emission spectra (a) and excitation spectra (b) of **1Eu** and **2Tb**, their dehydrated and rehydrated phases. For the as-prepared, dehydrated, and rehydrated samples, the measurement was performed under the same instrumental conditions (slits, scanning speed, etc.) at room temperature. The excitation wavelength for emission spectra is 394 nm for Eu and 330 nm for Tb, and the monitor wavelength for excitation spectra is 617 nm for Eu and 545 nm for Tb, respectively.

330 nm, with emissions at 494, 545, 587, and 621 nm assigned to $^5D_4 \rightarrow {}^7F_J$ ($J = 6, 5, 4, 3$) transitions of Tb^{3+}.[19] The material shows a change in its luminescence property similar to that of **1Eu** upon the de- and rehydration. It is interesting to observe this large intensity decrease in luminescence upon the dehydration and its recovery upon rehydration for the two porous luminescent materials, where water molecules in fact enhance the luminescence but not quench it, as what is usually believed[20] and observed in other lanthanide PMOFs.[9a,21] This interesting reverse might relate to the amorphous feature of the dehydrated phases, where the surrounding of Ln^{3+} ion becomes soft probably due to (a) the existence of a large number of defects or hanging bonds in the dehydrated materials and (b) the loss of the secondary coordination sphere around Ln^{3+} ion, thus greatly enhancing the radiationless process.[22] When rehydrated, the materials rebuild the original structure and recover their crystallinity, and the surrounding of Ln^{3+} becomes stiff again, and thus recovery of their luminescence is observed.

Conclusion

In summary, we have demonstrated that two porous luminescent frameworks of Eu and Tb could be obtained by the hydrothermal method employing the lanthanide ion, fumarate, and oxalate. They possess oxalate pillared lanthanide−fumarate layers with crossed channels for accommodation of guest water. The materials exhibited framework dynamics upon several cycles of dehydration and rehydration, and a reversible large change in their luminescence intensities upon de-/rehydration, where water in fact enhances the luminescence. This unusual reverse role of water is probable because the environment around lanthanide ion was softened in the amorphous dehydrated phases while it recovered stiffness upon rehydration. The significant luminescence changes upon de-/rehydration render the materials potential application for sensing water. Future work will investigate the detailed characteristics of the luminescent property and its dependence on the guest and the material crystallinity, proving the proposed de-/rehydration mechanism, as well as studying other Ln systems.

Acknowledgment. We thank Prof. Ling-Dong Sun and Prof. Chun-Hua Yan for valuable discussions on luminescence. Financial support from the National Natural Science Foundation of China (20571005, 20221101, 20490210) and the National Basic Research Program of China (2006CB601102) is gratefully acknowledged.

Supporting Information Available: Figures S1−S3 and an X-ray crystallographic file in CIF format. This material is available free of charge via the Internet at http://pubs.acs.org.

IC061833E

(19) For example: Singh, U. P.; Tyagi, S.; Sharma, C. L.; Görner, H.; Weyhermüller, T. *J. Chem. Soc., Dalton Trans.* **2002**, 4464 and refs 4−6 therein.

(20) (a) Horrocks, W. D., Jr.; Sudnick, D. R. *J. Am. Chem. Soc.* **1979**, *101*, 334. (b) Haas, Y.; Stein, G. *J. Phys. Chem.* **1971**, *75*, 3668. (c) Alpha, B.; Lehn, J.-M.; Mathis, G. *Angew. Chem., Int. Ed. Engl.* **1987**, *26*, 266.

(21) (a) Reineke, T. M.; Eddaoudi, M.; Fehr, M.; Kelley, D.; Yaghi, O. M. *J. Am. Chem. Soc.* **1999**, *121*, 1651. (b) de Lill, D. T.; Gunning, N. S.; Cahill, C. L. *Inorg. Chem.* **2005**, *44*, 258.

(22) Blasse, G.; Grabmaier, B. C. *Luminescent Materials*; Springer-Verlag: Berlin, Germany, 1994; Chapter 4.